THE JOURNAL OF PHYSICAL CHEMISTRY C LETTERS

2008, *112,* 11086–11089
Published on Web 06/20/2008

The Real Structure of Naturally Chiral Cu{643}

Ashleigh E. Baber,[†] Andrew J. Gellman,[‡] David S. Sholl,[§] and E. Charles H. Sykes*,[†]

Department of Chemistry, Tufts University, Medford, Massachusetts 02155-5813, Department of Chemical Engineering, Carnegie Mellon University, Pittsburgh, Pennsylvania 15213, and Department of Chemical & Biomolecular Engineering, Georgia Institute of Technology, Atlanta, Georgia 30332

Received: April 24, 2008; Revised Manuscript Received: May 23, 2008

Achiral metals can be cut, polished, and cleaned in such a way that they are terminated by surfaces on which all of the kink sites along the step edges are of the same chirality. The most studied of these surfaces is the {643} facet of Cu, which has been shown to interact enantiospecifically with chiral molecules. In order to fully exploit the potential of these surfaces for enantioselective chemistry, elucidating an atomic-scale picture of the active sites is crucial. Low-temperature scanning tunneling microscopy was used to study the structure of a Cu{643} crystal that had been thermally roughened at 1000 K. Images recorded at 78 K revealed that the real structure of Cu{643} is much more complex than the ideal structure. The number of chiral kink sites was quantified and compared to that expected for the ideal Cu{643} structure. Importantly, atomic resolution imaging revealed that the absolute chirality of the surface is preserved; however, thermal roughening led to a reduction in the absolute number of kinks.

Introduction

Chiral surfaces can be created by cutting single crystals of face-centered cubic (fcc) metals to expose surfaces with periodic arrays of steps, terraces, and kinks.[1] All high Miller index surfaces of fcc structures with Miller indices satisfying the criteria $h \neq k \neq l$ and $h... k... l \neq 0$ are chiral. Figure 1a shows an atomic model of an ideal {643} facet of an fcc metal. The origin of the chirality can be seen most easily by realizing that the kinks at the step edges are formed by the intersections of three *different* low Miller index microfacets. The direction of the progression from {111} to {100} to {110} microfacets dictates the handedness. By convention, fcc surfaces with clockwise rotation are denoted fcc{*hkl*}^{R} and those with counterclockwise rotation are denoted fcc{*hkl*}^{S}.[2,3] This description suggests that there are only six basic classes of kinks differentiated by whether the {111}, {110}, or {100} microfacets form the terrace, step, or kink. The surface of interest in this paper is the Cu{643}^{R} surface, which consists of narrow {111} terraces, step edges with a {100} orientation, and {110} kinks.

The real structures of chiral, high Miller index surfaces can be very different from those of the ideal bulk terminations shown in Figure 1a. Steps and kinked steps can undergo thermal roughening in which atomic diffusion results in the coalescence of kinks or even step bunching to form low Miller index facets.[4] Figure 1b shows an atomic model of a thermally roughened fcc {643} surface in which the average step length between kinks is longer than that on the ideal surface and there are fewer kink sites. Although the net chirality of the surface is retained after roughening, the roughened surface defines a range of potential step edge sites for molecular adsorption with varying local environments. This inhomogeneity in the kinds of sites that exist on the surface presents a challenge to efforts to model adsorption or catalysis on these surfaces.[5,6]

There is a growing body of data revealing the enantioselective properties of naturally chiral metal surfaces.[2,3,7–16] From the perspective of enantioselective chemistry, the most important results are those that reveal enantiospecific adsorption, desorption, and reaction energetics. The first experimental observations of enantioselectivity were made in 1999 by Attard et al. who discovered that the rates of electro-oxidation of D- and L-glucose depended on the chirality of the Pt{643} electrodes.[3] In terms of molecular interactions with naturally chiral surfaces, the best understood system is *R*-3-methylcyclohexanone adsorbed on the Cu{643}$^{R\&S}$ surfaces, which has been studied by Gellman and co-workers.[11,14,15] Temperature-programmed desorption of *R*-3-methylcyclohexanone on the Cu{643}$^{R\&S}$ surfaces revealed three peaks in the spectrum that correspond to desorption from the {111} terraces, the {100} straight step edges, and the {110} kink sites. The peak desorption temperatures of *R*-3-methylcyclohexanone from the Cu{643}^{R} and Cu{643}^{S} kink sites differ by $\Delta T_p = 3.5 \pm 0.8$ K, which equates to a desorption energy (ΔE_{des}) difference of $\Delta\Delta E_{des} \approx 1$ kJ/mol, or a difference in desorption rates of about 30% at room temperature. This result demonstrates that naturally chiral surfaces interact enantiospecifically with chiral adsorbates and that enantioselective catalysis and separations on naturally chiral surfaces are realistic goals. This work has now matured to the point that it has been possible to enantioselectively purify racemic 3-methylcyclohexanone on the naturally chiral Cu{643}$^{R\&S}$ surfaces.[15] Enantiospecific desorption kinetics have also been observed for R- and S-propylene oxide on the Cu{643}$^{R\&S}$ surfaces.[10]

* To whom correspondence should be addressed. E-mail: charles.sykes@tufts.edu.
[†] Tufts University.
[‡] Carnegie Mellon University.
[§] Georgia Institute of Technology.

10.1021/jp803601b CCC: $40.75

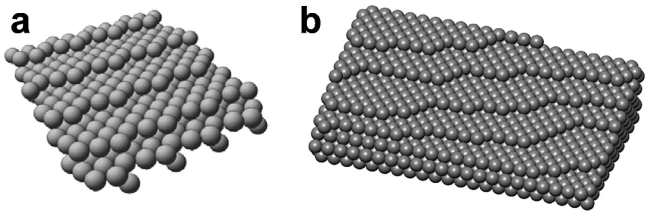

Figure 1. Schematic of ideal and thermally roughened {643} surfaces. Figure 1a shows that the ideal termination of an fcc crystal along the {643} plane exposes two-atom steps with single atom kinks. The real structures of chiral surfaces, however, can be very different from those of the ideal bulk terminations. Steps and kinked steps can undergo thermal roughening in which atomic diffusion results in the coalescence of kinks as depicted in Figure 1b.

Atomistic simulations by Sholl et al. were the first results to indicate that enantiospecific adsorption energetics could be observed on naturally chiral metal surfaces.[6–9,17] Those simulations used an empirical potential for the physisorption of alkanes on Pt surfaces.[18] Simulations of adsorption on thermally roughened Pt{643} surfaces show that although roughening reduces the density of kinks on a chiral surface it does not remove its net chirality.[4,6] More recently, density functional theory calculations have been used to examine enantiospecific chemisorption on chiral surfaces.[19–21]

Although several enantiospecific properties have been demonstrated on a number of naturally chiral metal surfaces, one of the critical limitations to our further understanding of these enantiospecific phenomena is the lack of a clear picture of the types of chiral sites and the distributions of site types that exist on these surfaces. A few recent studies have used scanning tunneling microscopy (STM) to image chiral surfaces. A room-temperature STM study of Cu{643} revealed a high step density; however, due to atomic mobility, kink sites could not be imaged.[22] Another room-temperature study of Cu(5 8 90) revealed the presence of kinks and that the surface appeared to be thermally roughened.[23] This paper describes a low-temperature STM study of the Cu{643}^{R} crystal at 78 K. By cooling the surface quickly after an annealing procedure, we were able to perform an atomic-scale characterization and quantify the kink density present on the thermally roughened surface. Atomically resolved images allowed the true structure of kink sites to be revealed and the results are discussed in terms of the enantiospecific chemistry observed on the Cu{643} surface.[10,11,14,15]

Experimental Section

All STM experiments were performed in a low-temperature, ultrahigh vacuum (LT-UHV) microscope built by Omicron.[24] The Cu{643} sample was prepared with a cleaning and cooling procedure identical to that used by Gellman and co-workers.[10,14,15] Briefly, the crystal was Ar^+-sputtered (1.5 keV/10 μA) for 30 min followed by a 2 min anneal to 1000 K. Approximately 12 of these sputter/anneal cycles were performed upon receiving the crystal, followed by a further 2 sputter/anneal cycles between each STM experiment. After the final anneal, the crystal was transferred in less than 3 min in vacuum ($<5 \times 10^{-10}$ mbar) to the precooled STM chamber. In approximately 30 min, the sample cooled from room temperature to 78 K. All images were recorded at 78 K with etched W tips, and voltages refer to the sample bias. In order to make an accurate count of the kink sites/nm^2 on the Cu{643} surface, it was necessary to precisely calibrate the STM images. This was achieved by using atomically resolved images of Au{111} to calibrate the x and y scanners and then cross-checking this calibration by comparing with measurements of the atomically resolved terraces of Cu{643}.

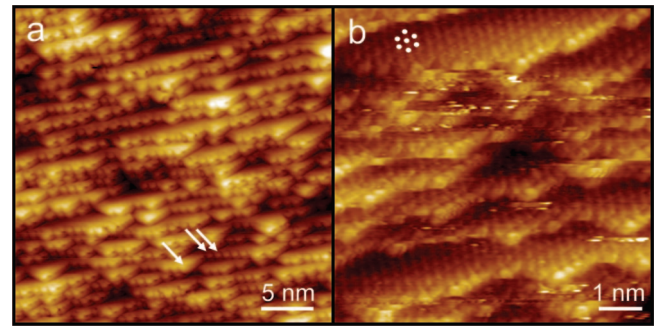

Figure 2. Figure 2a shows an STM image of the chiral Cu{643} surface. Terraces, steps, and kink sites are observed. The white arrows point to 3 kink sites. Figure 2b shows an atomically resolved image of Cu{643}. The 111 packing of Cu atoms on the terraces is highlighted by white circles, and the atoms at the step edges appear slightly larger than their neighbors in the terraces. Image conditions: (1a) $V = -0.3$ V, $I = 0.5$ nA; (1b) $V = -0.3$ V, $I = 0.09$ nA.

Results and Discussion

Figure 2a shows a typical STM image of the Cu{643} sample. Terraces, step edges, and kinks are visible. The terraces are between 0.5 and 4 nm in width perpendicular to the step edge, and are typically many tens of nanometers in length. The step heights are all 0.21 ± 0.01 nm, in exact agreement with the monatomic step heights on Cu{111}. Kink sites are highlighted by white arrows in Figure 2a and have a rounded appearance. Images of this quality could be obtained routinely when scanning the Cu{643} surface.

Atomically resolved images of the Cu{643} surface were much harder to acquire. The regular procedure for obtaining atomically resolved STM images is to find a large terrace away from step edges on which to tune the scanning and tunneling parameters until atomic resolution is acquired. However, the largest terraces on Cu{643} measure no more than a few nanometers in length; therefore, this technique was not feasible. We found that the optimal procedure for preparing tips that yield atomic resolution was by applying 10 V pulses to the tip during scanning, then moving to a new area of the surface. This procedure was repeated until atomically resolved images were obtained.

Figure 2b shows an atomically resolved area of the surface. It is obvious from this STM image that the atoms of the terraces are hexagonally packed, as highlighted by the white circles. It is also apparent from this data that step edge atoms are imaged slightly larger than the terrace atoms and that those atoms forming the obtuse kinks are the largest of all. Atoms at step edges have fewer nearest neighbors and different electronic properties from terrace atoms.[25,26] Their positions are also slightly perturbed from the expected lattice sites.[27] These facts mean that step edge atoms are often imaged differently than terrace atoms by STM.

The next stage of the study was aimed at quantifying the number of kink sites per unit area. One consequence of thermal roughening is the loss of kink sites in favor of the growth of longer step edges. The schematic in Figure 3a demonstrates that there are two types of kink, namely, acute and obtuse kinks. The atom at the center of an acute kink has 8 nearest neighbors, whereas atom at the center of an obtuse kink has 6 nearest neighbors. It is apparent from our STM images that the atom forming the obtuse kink is the most pronounced in the STM

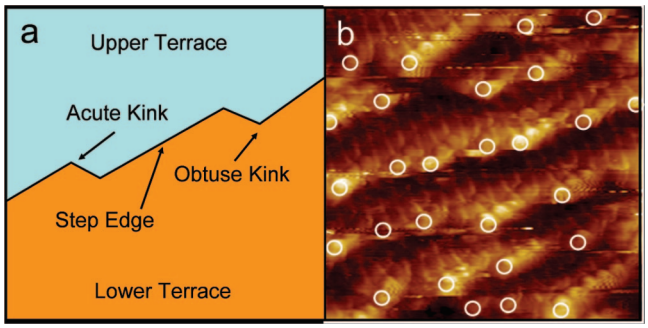

Figure 3. Figure 3a shows a schematic of terraces, step edges, and the two types of kink sites on chiral surfaces. Figure 3b shows an atomically resolved image of Cu{643} on which only the obtuse kink sites have been highlighted. Image conditions: $V = -0.3$ V, $I = 0.09$ nA.

TABLE 1: Experimental Results Quantifying the Number of Obtuse Kinks Per Unit Length along Step Edges and Per Unit Area on the Thermally Roughened Cu{643} Surface[a]

	atomic images	larger images	ideal Cu{643}
kinks/nm	1.1 ± 0.3	1.3 ± 0.1	1.46
kinks/nm^2	1.7 ± 0.2	1.8 ± 0.1	2.03

[a] The density of kinks is lower than that expected for the ideally terminated Cu{643} surface.

images, as would be expected because of its low coordination number.[25,26] Figure 3b shows such an STM scan in which each obtuse kink in the image is labeled with a white circle.

In order to quantify the number of kinks per unit area present on the thermally roughened Cu{643} surface, we recorded a set of images of different areas of the surface. This set of images contained both smaller, atomically resolved images (Figure 2b) and larger ones in which steps and kinks but not atoms could be resolved (Figure 2a). In all, over 1800 kinks in > 1000 nm^2 of STM images were counted. The number of obtuse kinks per unit length along a step edge and number of kinks per square nanometer was counted in both the atomically resolved and larger images. The choice of counting obtuse kinks stems from the fact that they are the most apparent in the STM images. By symmetry, for every obtuse kink there is an acute kink; therefore, quantifying one type of kink also defines the quantity of the other type of kink. Table 1 shows the results of the analysis of both the atomically resolved images and the larger ones.

The larger error bars for the atomically resolved images stems from the fact that the data set contained many more large images and, therefore, the standard deviation in counting kinks in the larger images was lower.

Thermal roughening of the Cu{643} surface is consistent with the results of temperature-programmed desorption (TPD) studies of the *R*-3-methylcyclohexanone from the surface.[14] As mentioned, the three desorption features observed during TPD of *R*-3-methylcyclohexanone can be assigned to molecules desorbing from the {111} terraces at ~230 K, molecules desorbing from the straight step edges at 345 K, and molecules desorbing from the chiral kink sites at 385 K. These features suggest that ~40% of the *R*-3-methylcyclohexanone desorbs from the kinks, 35% from the steps, and 25% from the terraces.[14] If the real surface had the ideal structure of the Cu{643} termination, as shown in Figure 1a, it is very difficult to imagine that the terraces are wide enough or the steps long enough to accommodate *R*-3-methylcyclohexanone adsorption at any sites other than the kinks. Observation of molecular desorption from the terraces and steps is entirely consistent with desorption from a thermally roughened surface, exposing wide terraces and long step edges.

In trying to draw connections between the structure of the clean roughened Cu{643} surface and the structure of the surface with adsorbed *R*-3-methylcyclohexanone, it is important to bear in mind the fact that molecular adsorption can influence surface structure. This has been observed many times in many adsorbate−substrate combinations but has also been observed for *R*-3-methylcyclohexanone adsorption on the Cu{533} surface at room temperature.[28] During adsorption of *R*-3-methylcyclohexanone at room temperature, the straight {100} step edges of the Cu{533} surface are roughened to induce the formation of kinks. This roughening does not seem to occur during adsorption at 90 K and subsequent heating during the TPD experiment. Nonetheless, one has to bear in mind the caveat of adsorbate-induced restructuring before trying to make quantitative connections between the roughened structure of the clean Cu{643} surface and the real structure of the surface modified by *R*-3-methlycyclohexanone adsorption.

Conclusions

A low-temperature STM study revealed that the real structure of Cu{643} deviates significantly from the expected ideal surface termination. Thermal roughening leads to the creation of longer step edges, wider terraces, and the coalescence of kink sites. Importantly, atomic resolution imaging showed that the absolute chirality of the surface is preserved, but thermal roughening leads to a reduction in the absolute number of kinks (1.8 ± 0.1 kinks/nm^2 as opposed to 2.03 kinks/nm^2 for the ideal structure).

Supporting Information Available: Tables showing the experimentally measured kink density. STM image of a large area of the Cu{643} surface (67.8×75.3 nm^2) with roughness measurements. This information is available free of charge via the Internet at http://pubs.acs.org.

Acknowledgment. We thank the NSF (Grant no. 0717978) for support of this research. A.E.B. and E.C.H.S. thank the ACS-PRF (Grant no. 45256-G5), Research Corporation, and the Beckman Foundation for additional support. A.E.B. thanks the DOEd for a GAANN fellowship.

References and Notes

(1) McFadden, C. F.; Cremer, P. S.; Gellman, A. J. *Langmuir* **1996**, *12*, 2483.
(2) Ahmadi, A.; Attard, G.; Feliu, J.; Rodes, A. *Langmuir* **1999**, *15*, 2420.
(3) Attard, G. A.; Ahmadi, A.; Feliu, J.; Rodes, A.; Herrero, E.; Blais, S.; Jerkiewicz, G. *J. Phys. Chem. B* **1999**, *103*, 1381.
(4) Asthagiri, A.; Feibelman, P. J.; Sholl, D. S. *Top. Catal.* **2002**, *18*, 193.
(5) Bhatia, B.; Sholl, D. S. *J. Chem. Phys.*, in press.
(6) Power, T. D.; Asthagiri, A.; Sholl, D. S. *Langmuir* **2002**, *18*, 3737.
(7) Sholl, D. S.; Asthagiri, A.; Power, T. D. *J. Phys. Chem. B* **2001**, *105*, 4771.
(8) Power, T. D.; Sholl, D. S. *Top. Catal.* **2002**, *18*, 201.
(9) Sholl, D. S. *Langmuir* **1998**, *14*, 862.
(10) Horvath, J. D.; Gellman, A. J. *J. Am. Chem. Soc.* **2001**, *123*, 7953.
(11) Gellman, A. J.; Horvath, J. D.; Buelow, M. T. *J. Mol. Catal. A* **2001**, *167*, 3.
(12) Attard, G. A. *J. Phys. Chem. B* **2001**, *105*, 3158.
(13) Attard, G. A.; Harris, C.; Herrero, E.; Feliu, J. *Faraday Discuss.* **2002**, *121*, 253.
(14) Horvath, J. D.; Gellman, A. J. *J. Am. Chem. Soc.* **2002**, *124*, 2384.
(15) Horvath, J. D.; Koritnik, A.; Kamakoti, P.; Sholl, D. S.; Gellman, A. J. *J. Am. Chem. Soc.* **2004**, *126*, 14988.
(16) Rampulla, D. M.; Francis, A. J.; Knight, K. S.; Gellman, A. J. *J. Phys. Chem. B* **2006**, *110*, 10411.
(17) Rankin, R. B.; Sholl, D. S. *Langmuir* **2006**, *22*, 8096.
(18) Stinnett, J. A.; Madix, R. J.; Tully, J. C. *J. Chem. Phys.* **1996**, *104*, 3134.

(19) Bhatia, B.; Sholl, D. S. *Angew. Chem., Int. Ed.* **2005**, *44*, 7761.
(20) James, J. N.; Sholl, D. S. *Curr. Opin. Colloid Interface Sci.* **2008**, *13*, 60.
(21) Sljivancanin, Z.; Gothelf, K. V.; Hammer, B. *J. Am. Chem. Soc.* **2002**, *124*, 14789.
(22) Zhao, X. Y.; Perry, S. S. *J. Mol. Catal. A* **2004**, *216*, 257.
(23) Giesen, M.; Dieluweit, S. *J. Mol. Catal. A* **2004**, *216*, 263.
(24) Becker, T.; Hövel, H.; Tschudy, M.; Reihl, B. *Appl. Phys. A: Mater. Sci. Process.* **1998**, *66*, S27.
(25) Avouris, P.; Lyo, I. W.; Molinasmata, P. *Chem. Phys. Lett.* **1995**, *240*, 423.
(26) Smoluchowski, R. *Phys. Rev.* **1941**, *60*, 661.
(27) Wei, C. Y.; Lewis, S. P.; Mele, E. J.; Rappe, A. M. *Phys. Rev. B* **1998**, *57*, 10062.
(28) Zhao, X. Y.; Perry, S. S.; Horvath, J. D.; Gellman, A. J. *Surf. Sci.* **2004**, *563*, 217.

JP803601B